applied sciences

MDPI

Article

Generation of Cold Magnetized Relativistic Plasmas at the Rear of Thin Foils Irradiated by Ultra-High-Intensity Laser Pulses

Artem V. Korzhimanov

Federal Research Center, Institute of Applied Physics, Russian Academy of Sciences, 603950 Nizhny Novgorod, Russia; artem.korzhimanov@ipfran.ru

Abstract: A scheme to generate magnetized relativistic plasmas in a laboratory setting is proposed. It is based on the interaction of ultra-high-intensity sub-picosecond laser pulses with few-micron-thick foils or films. By means of Particle-In-Cell simulations, it is shown that energetic electrons produced by the laser and evacuated at the rear of the target trigger an expansion of the target, building up a strong azimuthal magnetic field. It is shown that in the expanding plasma sheath, a ratio of the magnetic pressure and the electron rest-mass energy density exceeds unity, whereas the plasma pressure is lower than the magnetic pressure and the electron gyroradius is lower than the plasma dimension. This scheme can be utilized to study astrophysical extreme phenomena such as relativistic magnetic reconnection in laboratory.

Keywords: relativistic plasmas; magnetized plasmas ultra-high-intensity lasers; laboratory astrophysics; particle-in-cell simulations

check for updates

Citation: Korzhimanov, A.V. Generation of Cold Magnetized Relativistic Plasmas at the Rear of Thin Foils Irradiated by Ultra-High-Intensity Laser Pulses. *Appl. Sci.* **2021**, *11*, 11966. https://doi.org/10.3390/app112411966

Academic Editor: István B Földes

Received: 24 November 2021
Accepted: 14 December 2021
Published: 16 December 2021

Publisher's Note: MDPI stays neutral with regard to jurisdictional claims in published maps and institutional affiliations.

Copyright: © 2021 by the author. Licensee MDPI, Basel, Switzerland. This article is an open access article distributed under the terms and conditions of the Creative Commons Attribution (CC BY) license (https://creativecommons.org/licenses/by/4.0/).

1. Introduction

Recently, there has been an increased interest in the possibility of investigating processes characteristic of extreme astrophysical objects in laboratories using powerful laser systems [1,2]. In particular, much attention is paid to the study of the magnetic reconnection process, which is widely encountered in space. Typical experiments in this area use two nanosecond laser pulses with energies ranging from a few Joules to several kilojoules to irradiate a metal surface. As a result of the interaction, ablation of a heated substance takes place, in which azimuthal magnetic fields are self-generated due to the Biermann battery effect. Such magnetized expanding plumes may be arranged to collide with each other, initiating a reconnection of oppositely directed magnetic lines in an interaction region [3–7].

In most of the experiments carried out, however, the case of a nonrelativistic plasma was investigated. At the same time, magnetic reconnection in the relativistic regime is expected to occur in a vicinity of extreme astrophysical objects such as pulsars, magnetars, and active galactic nuclei. A key parameter in this case is a cold magnetization parameter, which is equal to a ratio of a magnetic pressure to an electron rest energy density $\sigma = B^2/(\mu_0 n_e m_e c^2)$, where B is the magnetic field induction; μ_0 is the magnetic constant; n_e, m_e are the concentration and mass of electrons, respectively; and c is the speed of light [8]. The case of the magnetized relativistic plasma corresponds to $\sigma > 1$, and until recently such values were unattainable in the laboratory.

In recent works, however, the $\sigma > 1$ regime was obtained by two methods. One of them is similar to the approach of non-relativistic experiments, but it used either a pair of 2 J, 40 fs laser pulses from the HERCULES facility, or 500 J, 20 ps pulses from the OMEGA EP facility [9]. The high power of laser pulses made it possible to attain intensities of the order of 10^{18}–10^{19} W/cm^2 at the focus, which, as is known, is sufficient for the energy of the electrons to become comparable to their rest energy [10]. As a result, a field of approximately 1 kT was generated in the expanding plasma plume, which made it possible to reach $\sigma \sim 10$. An integral property of the scheme used, however, was the high value

of a parameter $\beta = \mu_0 n_e k T_e / B^2$, equal to the ratio of the electron kinetic pressure to the magnetic pressure (here, k is the Boltzmann constant and T_e is the electron temperature). In the experiment, its value was estimated at $\beta \sim 50$. At the same time, in the aspect of astrophysical applications, a cold plasma with a dominant role of a magnetic field and $\beta \ll 1$ is usually considered.

The second method for achieving high degrees of magnetization in a laser-plasma experiment is based on the use of a picosecond laser pulse of a kilojoule energy level to generate a magnetic field in a microcoil [11]. When a coil was irradiated with laser radiation at opposite ends, counterstreaming currents of the order of 1 MA were generated in it, which led to the creation of antiparallel fields of magnitude above 1 kT. According to estimates, the experiment reached $\sigma \sim 20$–100 at $\beta \sim 0.01$–0.1. The main disadvantage of such experiments is a hard accessibility of such laser systems.

Other methods of organizing relativistic magnetic reconnection have been theoretically proposed as alternative approaches. For example, in [12–17] it is proposed to observe an antiparallel configuration of magnetic fields during a parallel propagation of two ultrashort superintense laser pulses in transparent plasma. In plasma wakefields generated by them, the azimuthal magnetic field is observed. When two wakefields come into contact, for example, when they gradually expand in plasma with a negative density gradient, those fields begin to annihilate. The disadvantage of this method is that the electrons in the interaction region are relativistic, and their Larmor radii exceed a size of the region of localization of magnetic fields. That is the reconnection is observed only in the electron diffusion region in the very vicinity of an X-point.

Finally, in [18], the authors propose using micro-slabs irradiated with laser pulses along a surface to observe relativistic magnetic reconnection. It was shown numerically that when using a femtosecond laser pulse of multi-terawatt power, $\sigma \sim 1$ can be achieved at $\beta \sim 0.1$, and when the power is increased to a petawatt level, $\sigma > 100$ can be achieved. The main difficulty in the experimental implementation of such a scheme is the need to use high-contrast laser pulses and precise targeting of a relatively tightly focused pulse to the end of a slab of submicron thickness.

In this paper, we propose another method for generating cold ($\beta \sim 0.1$) magnetized ($\sigma \sim 10$) relativistic plasma, which is based on the interaction of powerful subpicosecond pulses with thin targets. As is known, the interaction of relativistically intense radiation with the surface leads to efficient generation of beams of energetic electrons injected by the field into the target [19–21]. These electrons, possessing relativistic energies, freely pass through targets up to several tens of microns thick. Escaping from the back side, they are decelerated by an emerging charge separation field and initiate ionization of the rear surface of the target and the expansion of the resulting plasma. As a result, a plasma sheath is formed, with electrons heated to relativistic temperatures and a laminar flow of cold ions [22].

Continuing escaping electron bunches form a current on the axis of the sheath and generate an azimuthal magnetic field [23]. At low laser pulse intensities and durations, this field does not significantly alter the expansion dynamics, although it can lead to the observed changes in the spectrum of the expanding ions. Recently, however, it was discovered that for pulses of several hundred femtoseconds duration and intensity above 10^{20} W/cm^2, the magnetic field is sufficient to magnetize the electrons and thereby appreciably slow down the expansion of the plasma [24,25].

In this work, we studied in more detail the properties of the resulting plasma and found that conditions for a cold magnetized relativistic plasma are realized in it, allowing using this mechanism for observing relativistic magnetic reconnection under laboratory conditions.

2. Methods

An analysis of a formation of the magnetized plasma during the interaction of laser radiation with thin dense targets was carried out by numerical simulation of a complete

self-consistent system of Maxwell equations for electromagnetic fields and kinetic Vlasov equations for plasma species by means of a particle-in-cell method using the PICADOR software package [26]. Modeling was carried out in two-dimensional geometry. The length of the box was selected in the range from 280 to 380 μm, depending on the intensity and duration of the laser pulse, so that by the end of the simulation the plasma did not reach the right boundary. The box width was 80 μm. A grid step along both axes was 0.02 μm. The calculation time was 3000 fs and the time step was 0.02 fs. Absorbing boundary conditions were used at all boundaries both for particles and fields. The number of particles in the cell at the initial moment of time was 200.

An aluminum foil with a thickness of 2 μm was used as the target. It was located at a distance of 30 μm from the left boundary of the box. Ions were pre-ionized to the Al^{9+} state. Their concentration at the initial moment of time was 5×10^{22} cm^{-3}. The boundaries of the target were initially assumed to be perfectly sharp. A layer of fully ionized hydrogen with a thickness of 0.02 μm was added to the rear surface of the target, which imitated a natural contamination of the target surface, and also accelerated the expansion of the plasma due to the smaller mass of protons compared to the mass of aluminum ions.

The 2D simulations were carried out so that the linearly polarized laser light was in the plane of the simulations. The beam was incident onto the target from the left along the normal to the surface and focused into a spot 4 μm in diameter at FWHM (Full Width at Half Maximum). The calculations were performed with pulses with a duration of 100, 400, 700, and 1000 fs at FWHM. The results for pulses with the duration of 400 fs and longer are in qualitative agreement with each other so only qualitatively different cases of 100 fs and 700 fs are presented in the paper. The pulse envelope in both coordinates was a Gaussian.

The noisy distributions of electron density, electron energy density and magnetic field obtained as a result of modeling were smoothed by a Gaussian filter with a width of 0.2 μm. All transformations have then been carried out on smoothed distributions. To obtain a magnetic field gradient, we used a convolution of the initial distribution of the magnetic field with the first derivative of the Gaussian function in both directions with the same width of 0.2 μm.

3. Results

Figure 1 shows the time evolution of the electron density n_e, the electron temperature T_e (obtained as a ratio of the local kinetic energy density of electrons to their concentration) and the transverse component of the magnetic field B_z at different times for a pulse with a duration of 700 fs and an intensity of 10^{20} W/cm^2.

It can be seen that at the beginning (Figure 1d,e) the target is deformed under the action of radiation and a noticeable pre-plasma layer is formed in the region $x < 0$ μm, which enhances absorption of radiation. Later the interaction takes the form of a so-called "hole-boring" which enhances the absorption even more. On the rear side of the target, the expulsion of the energetic electrons is observed. It triggers the expansion of the plasma and the formation of the plasma sheath. At a later moment in time (Figure 1g–i), an increase in the azimuthal magnetic field is observed in the formed plasma sheath. With increasing intensity, the magnitude of the generated magnetic field also grows, reaching a maximum at the moment when the maximum of the laser pulse arrives at the target (Figure 1j–l).

At this moment, the magnetic field at its peak reaches a value of the order of 400 MG, and is of the order of 100 MG in most of the plasma sheath. Note that the electron concentration in the same region is in the range 10^{20}–10^{21} cm^{-3}. As for the electron temperature, a high-energy electron current is observed on the sheath axis; however, to the side of it, the electron temperature is much lower, and in a significant region near the target, it is significantly below the relativistic value $kT_e < mc^2$. Due to the fact that in such a plasma there are no effective mechanisms for cooling electrons, then, most likely, these cold electrons were drawn out by a cold reverse current to compensate for the charge of hot electrons that had sufficient energy to leave the interaction region.

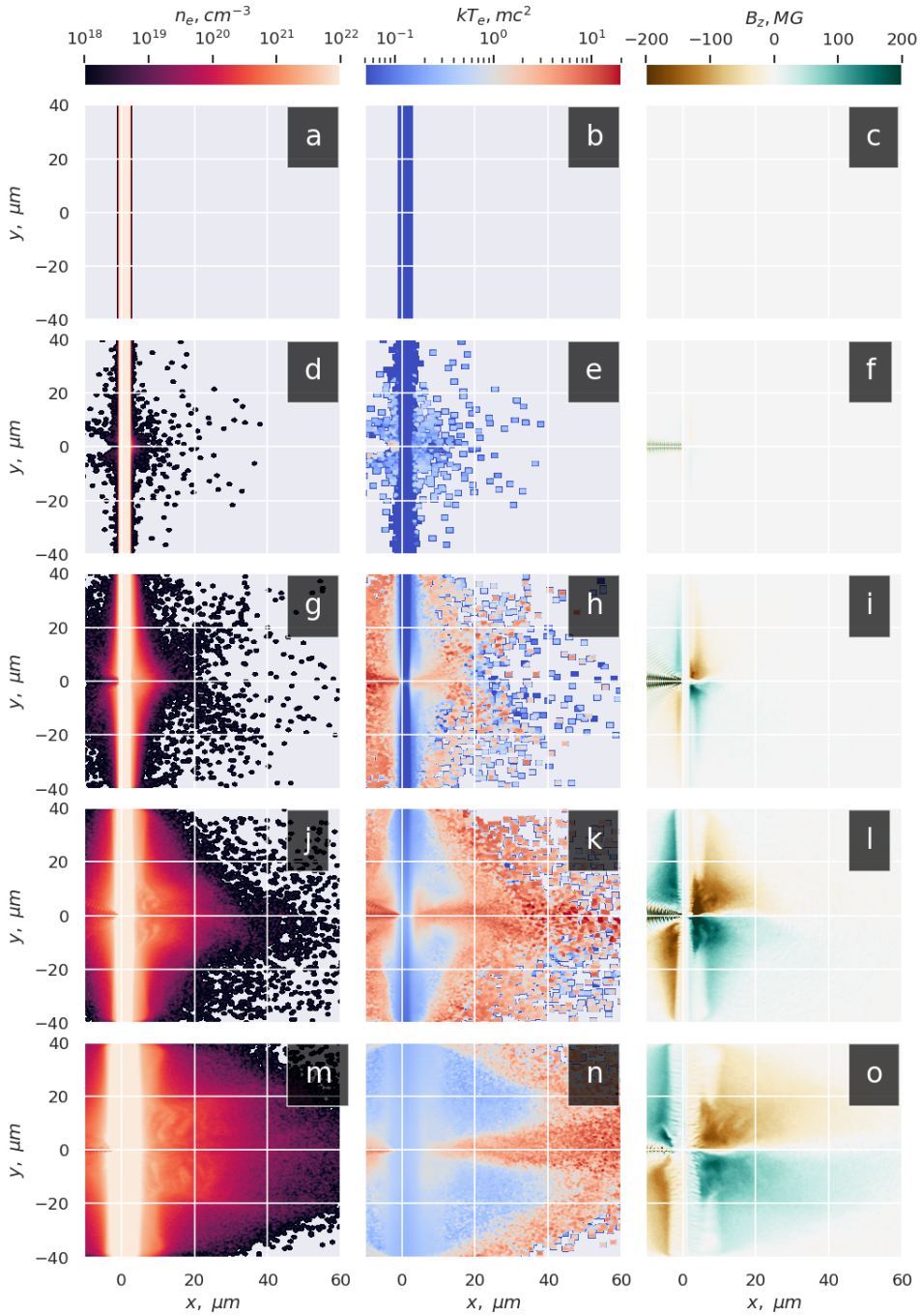

Figure 1. Distributions of electron concentration (left column), electron temperature (central column) and transverse magnetic field (right column) at (**a–c**) $t = 0$ fs, (**d–f**) $t = 500$ fs, (**g–i**) $t = 1000$ fs, (**j–l**) $t = 1500$ fs, and (**m–o**) $t = 2000$ fs after start of the simulation. The parameters of the simulation are in the text.

At later times, the plasma continues to expand and cool down a little, but the magnetic field is dissipating slowly and changes in magnitude insignificantly. An interesting feature is that, as follows from the performed calculations, the magnitude of the magnetic field at later times is practically independent of the intensity of the laser radiation. This can be seen from Figure 2, which shows a time dependence of the peak value of the magnetic field for different intensities of the laser pulses with fixed duration. Although the field value at

the maximum of the laser pulse increases with intensity, it relaxes to an almost identical value of about 100 MG after the pulse leaves.

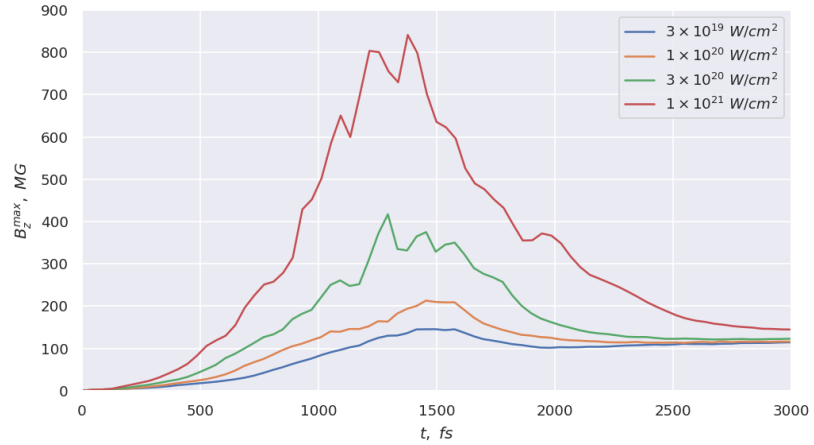

Figure 2. Time evolution of the peak magnetic field generated in the expanding plasma sheath for different laser intensities.

Let us now turn to an analysis of the main parameters of the resulting plasma. Figure 3 shows the distributions of the previously introduced parameters $\beta = \mu_0 n_e k T_e / B_z^2$ and $\sigma = B_z^2 / \mu_0 n_e m_e c^2$, and also a quantity $\delta = R_L / (B_z / |\nabla B_z|)$, equal to the ratio of the Larmor radius $R_L = \sqrt{k T_e / m_e B_z^2}$ to a characteristic scale of the magnetic field variation $L_B = B_z / |\nabla B_z|$. The analysis of δ is important because for effective plasma magnetization it is not enough to have a sufficiently large magnetic field, but it is also required that the electrons can make a full revolution in the magnetic field before they leave the region of their localization. This can be a limiting factor in femtosecond laser plasma due to the small interaction volume and high gradients of the generated magnetic field. In particular, this is one of the limiting factors for the generation of magnetized plasma by pulses with a duration of less than 100 fs.

Within the discussed range of parameters, however, such a problem does not arise, although, as can be seen from Figure 3, the region in which $\delta < 1$ (depicted in blue at Figure 3c,f,i) turns out to be remarkably smaller than the region in which $\sigma > 1$ (depicted in red at Figure 3b,e,h) and $\beta < 1$ (depicted in blue at Figure 3a,d,g).

Despite this, it can be seen that at the beginning of the interaction, the plasma is non-magnetized (Figure 3b). However, by the arrival of the radiation maximum, a noticeable region of cold magnetized plasma appears (Figure 3d,e), which further begins to expand (Figure 3g,h). The achieved values of σ are relatively small and do not exceed 10.

Achievement of larger values can be expected at higher intensities; therefore, we performed calculations in the range of intensities 3×10^{19}–10^{21} W/cm^2. The results are shown in Figure 4. It can be seen that at low intensities (Figure 4a–c) no magnetized plasma is formed. Although there is a noticeable region of low electron temperature in the sheath, the magnetic field is too weak to exceed the rest energy density of the electrons. With an increase in intensity, the plasma expands with increasingly high speeds, which is in accordance with the theory of collisionless plasma expansion into vacuum [27,28]. The magnitude of the generated magnetic fields also increases, and a significant region of cold magnetized plasma is formed. In this case, the degree of magnetization also increases and reaches $\sigma \sim 10$ for 10^{21} W/cm^2. Simultaneously, the value of δ remains small.

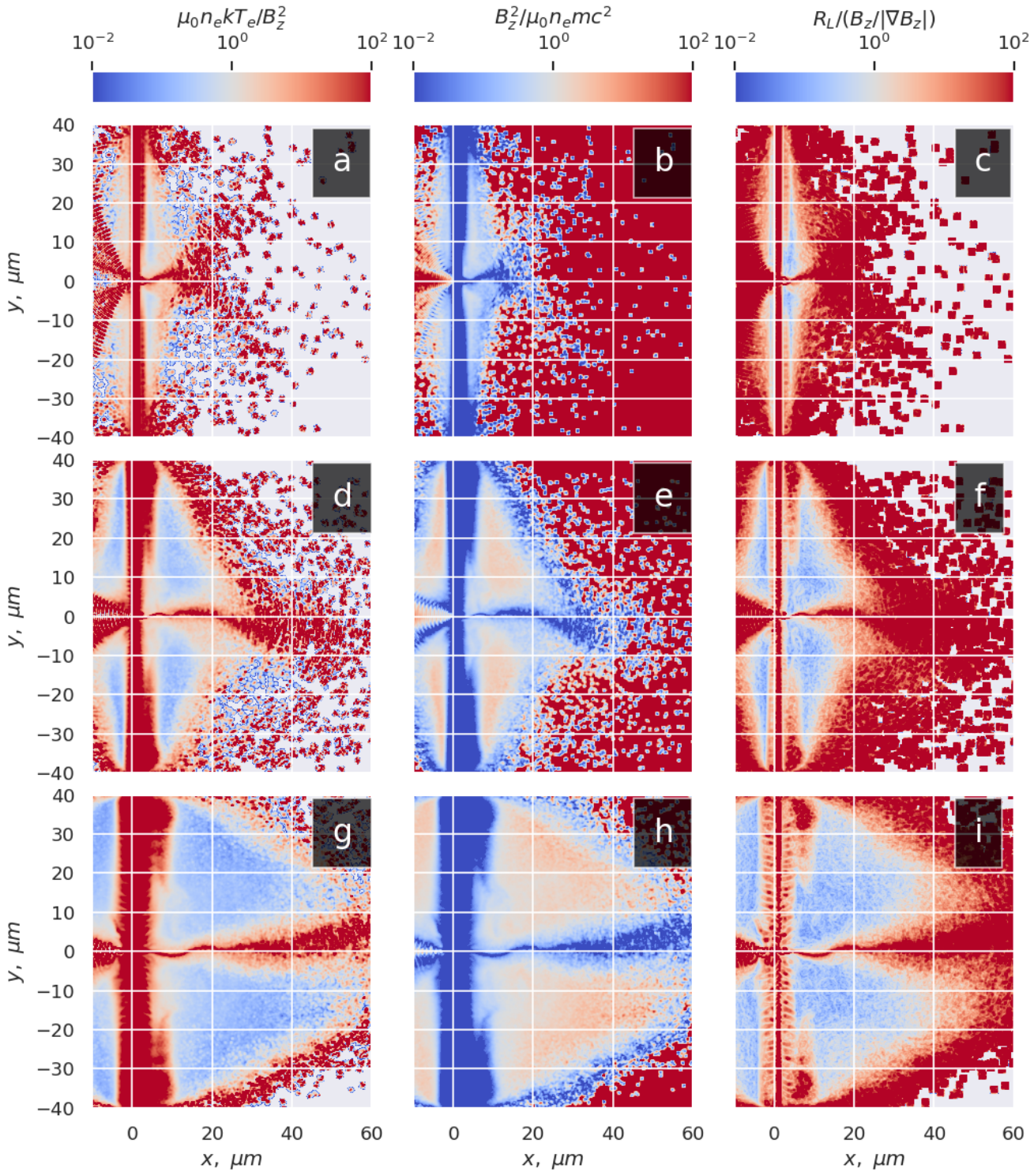

Figure 3. Distributions of β parameter (left column), σ parameter (central column) and δ parameter (right column) at (**a**–**c**) $t = 1000$ fs, (**d**–**f**) $t = 1500$ fs, and (**g**–**i**) $t = 2000$ fs after start of the simulation. The parameters of the simulation are the same as at Figure 1.

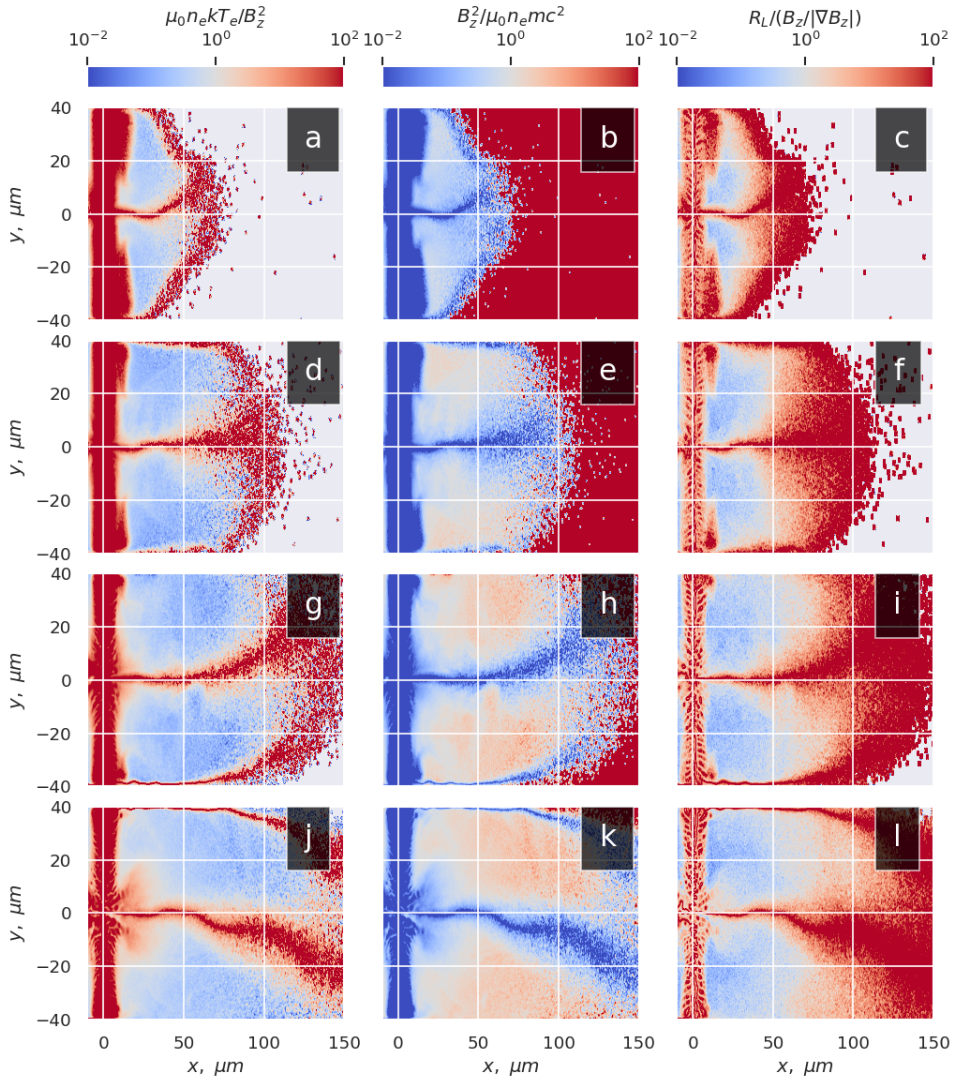

Figure 4. The same as at the Figure 3 but at $t = 2500$ fs after start of the simulations for laser intensities of (**a**–**c**) 3×10^{19} W/cm^2, (**d**–**f**) 10^{20} W/cm^2, (**g**–**i**) 3×10^{20} W/cm^2, and (**j**–**l**) 10^{21} W/cm^2.

Furthermore, note that efficient magnetization of the expanding sheath was observed only for relatively long pulses with the duration exceeding 400 fs. The case of a shorter 100 fs pulse is shown at Figure 5. The shown instant of time is corresponding to a moment of a peak intensity arrival. For such a short laser pulse, even at the highest investigated intensity of 10^{21} W/cm^2, there is not enough time for the sheath to expand significantly (Figure 5a) and the electrons are still relativistically hot all over the sheath (Figure 5b), leading to high β parameter (Figure 5d). Moreover, despite the fact that the magnetic field is relatively high ($B_z \sim 500$ MG at the peak, which should be compared to 800 MG for the same intensity for 700 fs pulse as shown at Figure 2), the weakly expanded sheath is rather dense so that the magnetization parameter $\sigma < 1$ (Figure 5e). Finally, due to a small dimension of the sheath the parameter $\delta < 1$ as well (Figure 5f). An exact pulse duration sufficient to obtain the magnetized plasmas depends on the pulse intensity and likely on the details of interaction but it seems that in a wide set of parameters it lays somewhere between 100 and 500 fs.

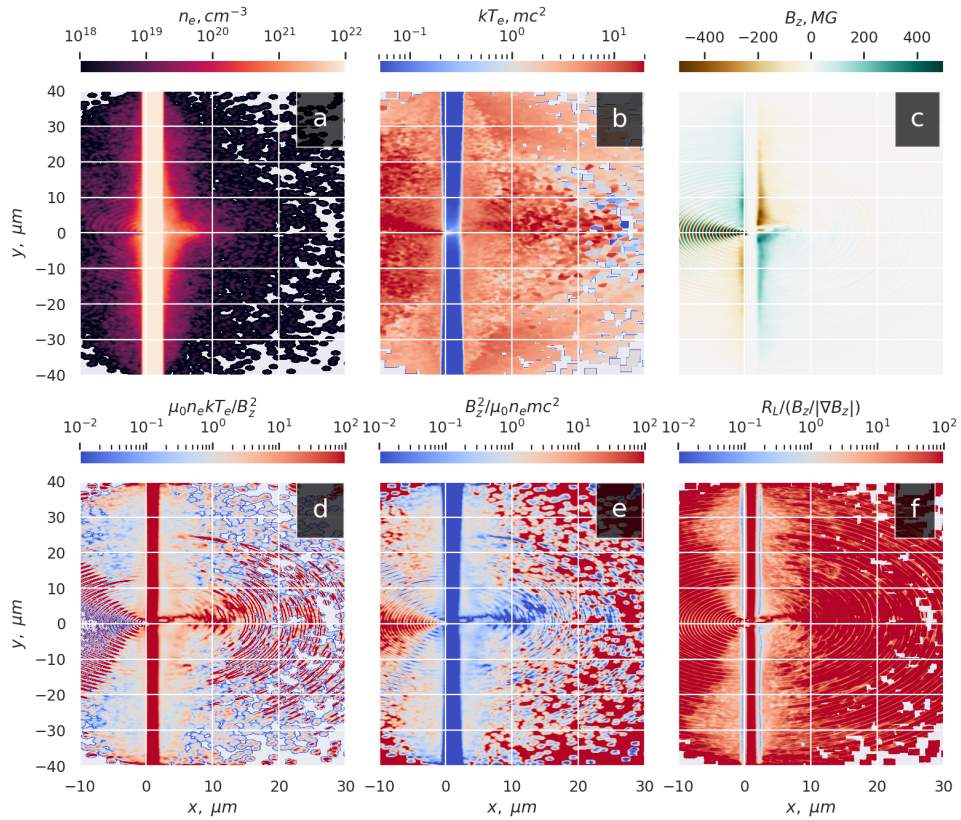

Figure 5. Distributions of (**a**) electron concentration, (**b**) electron temperature, (**c**) transverse magnetic field, (**d**) β parameter, (**e**) σ parameter, and (**f**) δ parameter in the case of 100 fs, 10^{21} W/cm^2 laser pulse at $t = 500$ fs after start of the simulation.

4. Discussion

Concluding, our numerical simulation showed that as a result of irradiation of thin (approximately a few microns thick) foils by relativistically intense laser pulses with a duration of several hundred femtoseconds, an expanding plasma sheath is formed on the rear side of the target, the conditions in which correspond to a cold magnetized plasma with parameters $\beta \sim 0.01$–0.1 and $\sigma \sim 1$–10. To create such conditions, an intensity higher than 10^{20} W/cm^2 and a pulse duration higher than 100–400 fs are required; conditions that are already available in experiments. To organize magnetic reconnection, two pulses are required, which are focused at a distance of about 50–100 μm from each other. This opens up new possibilities for the study of relativistic magnetic reconnection in the laboratory.

Additionally, we note that it can be expected that next-generation laser facilities carrying hundreds of joules in sub-picosecond pulses will be able to create conditions in which the effects of radiation cooling and generation of electron–positron pairs become observable. Recently, it has been proposed that they can play an important role in relativistic magnetic reconnection [29,30]. The study of such a possibility is an interesting possible subject of a future work.

Funding: This research was supported by Center of Excellence "Center of Photonics" funded by The Ministry of Science and Higher Education of the Russian Federation, contract 075-15-2020-906. The simulations were performed on resources provided by the Joint Supercomputer Center of the Russian Academy of Sciences.

Data Availability Statement: The data that support the findings of this study are available from the corresponding author upon reasonable request.

Conflicts of Interest: The author declares no conflict of interest.

References

1. Remington, B.; Drake, R.; Ryutov, D. Experimental astrophysics with high power lasers and Z pinches. *Rev. Mod. Phys.* **2006**, *78*, 755–807. [CrossRef]
2. Bulanov, S.V.; Esirkepov, T.Z.; Kando, M.; Koga, J.; Kondo, K.; Korn, G. On the problems of relativistic laboratory astrophysics and fundamental physics with super powerful lasers. *Plasma Phys. Rep.* **2015**, *41*, 1–51. [CrossRef]
3. Nilson, P.M.; Willingale, L.; Kaluza, M.C.; Kamperidis, C.; Minardi, S.; Wei, M.S.; Fernandes, P.; Notley, M.; Bandyopadhyay, S.; Sherlock, M.; et al. Magnetic Reconnection and Plasma Dynamics in Two-Beam Laser-Solid Interactions. *Phys. Rev. Lett.* **2006**, *97*, 255001. [CrossRef] [PubMed]
4. Fox, W.; Bhattacharjee, A.; Germaschewski, K. Fast Magnetic Reconnection in Laser-Produced Plasma Bubbles. *Phys. Rev. Lett.* **2011**, *106*, 215003. [CrossRef]
5. Fiksel, G.; Fox, W.; Bhattacharjee, A.; Barnak, D.H.; Chang, P.Y.; Germaschewski, K.; Hu, S.X.; Nilson, P.M. Magnetic Reconnection between Colliding Magnetized Laser-Produced Plasma Plumes. *Phys. Rev. Lett.* **2014**, *113*, 105003. [CrossRef] [PubMed]
6. Rosenberg, M.J.; Li, C.K.; Fox, W.; Zylstra, A.B.; Stoeckl, C.; Séguin, F.H.; Frenje, J.A.; Petrasso, R.D. Slowing of Magnetic Reconnection Concurrent with Weakening Plasma Inflows and Increasing Collisionality in Strongly Driven Laser-Plasma Experiments. *Phys. Rev. Lett.* **2015**, *114*, 205004. [CrossRef]
7. Matteucci, J.; Fox, W.; Bhattacharjee, A.; Schaeffer, D.B.; Moissard, C.; Germaschewski, K.; Fiksel, G.; Hu, S.X. Biermann-Battery-Mediated Magnetic Reconnection in 3D Colliding Plasmas. *Phys. Rev. Lett.* **2018**, *121*, 095001. [CrossRef] [PubMed]
8. Lyubarsky, Y.E. On the relativistic magnetic reconnection. *Mon. Not. R. Astron. Soc.* **2005**, *358*, 113–119. [CrossRef]
9. Raymond, A.E.; Dong, C.F.; McKelvey, A.; Zulick, C.; Alexander, N.; Bhattacharjee, A.; Campbell, P.T.; Chen, H.; Chvykov, V.; Del Rio, E.; et al. Relativistic-electron-driven magnetic reconnection in the laboratory. *Phys. Rev. E* **2018**, *98*, 043207. [CrossRef]
10. Mourou, G.; Tajima, T.; Bulanov, S. Optics in the relativistic regime. *Rev. Mod. Phys.* **2006**, *78*, 309–371. [CrossRef]
11. Law, K.F.F.; Abe, Y.; Morace, A.; Arikawa, Y.; Sakata, S.; Lee, S.; Matsuo, K.; Morita, H.; Ochiai, Y.; Liu, C.; et al. Relativistic magnetic reconnection in laser laboratory for testing an emission mechanism of hard-state black hole system. *Phys. Rev. E* **2020**, *102*, 033202. [CrossRef] [PubMed]
12. Gu, Y.J.; Klimo, O.; Kumar, D.; Bulanov, S.V.; Esirkepov, T.Z.; Weber, S.; Korn, G. Fast magnetic field annihilation driven by two laser pulses in underdense plasma. *Phys. Plasmas* **2015**, *22*, 103113. [CrossRef]
13. Gu, Y.J.; Yu, Q.; Klimo, O.; Esirkepov, T.Z.; Bulanov, S.V.; Weber, S.; Korn, G. Fast magnetic energy dissipation in relativistic plasma induced by high order laser modes. *High Power Laser Sci. Eng.* **2016**, *4*, e19. [CrossRef]
14. Gu, Y.J.; Klimo, O.; Kumar, D.; Liu, Y.; Singh, S.K.; Esirkepov, T.Z.; Bulanov, S.V.; Weber, S.; Korn, G. Fast magnetic-field annihilation in the relativistic collisionless regime driven by two ultrashort high-intensity laser pulses. *Phys. Rev. E* **2016**, *93*, 013203. [CrossRef] [PubMed]
15. Gu, Y.J.; Bulanov, S.S.; Korn, G.; Bulanov, S.V. Splitter target for controlling magnetic reconnection in relativistic laser plasma interactions. *Plasma Phys. Control. Fusion* **2018**, *60*, 044020. [CrossRef]
16. Gu, Y.J.; Pegoraro, F.; Sasorov, P.V.; Golovin, D.; Yogo, A.; Korn, G.; Bulanov, S.V. Electromagnetic Burst Generation during Annihilation of Magnetic Field in Relativistic Laser-Plasma Interaction. *Sci. Rep.* **2019**, *9*, 19462. [CrossRef]
17. Gu, Y.J.; Bulanov, S.V. Magnetic field annihilation and charged particle acceleration in ultra-relativistic laser plasmas. *High Power Laser Sci. Eng.* **2021**, *9*, e2. [CrossRef]
18. Yi, L.; Shen, B.; Pukhov, A.; Fülöp, T. Relativistic magnetic reconnection driven by a laser interacting with a micro-scale plasma slab. *Nat. Commun.* **2018**, *9*, 1601. [CrossRef] [PubMed]
19. Brunel, F. Anomalous absorption of high intensity subpicosecond laser pulses. *Phys. Fluids* **1988**, *31*, 2714–2719. [CrossRef]
20. Mulser, P.; Weng, S.M.; Liseykina, T. Analysis of the Brunel model and resulting hot electron spectra. *Phys. Plasmas* **2012**, *19*, 043301. [CrossRef]
21. Liseykina, T.; Mulser, P.; Murakami, M. Collisionless absorption, hot electron generation, and energy scaling in intense laser-target interaction. *Phys. Plasmas* **2015**, *22*, 033302. [CrossRef]
22. Wilks, S.C.; Langdon, A.B.; Cowan, T.E.; Roth, M.; Singh, M.; Hatchett, S.; Key, M.H.; Pennington, D.; MacKinnon, A.; Snavely, R.A. Energetic proton generation in ultra-intense laser-solid interactions. *Phys. Plasmas* **2001**, *8*, 542–549. [CrossRef]
23. Robinson, A.P.L.; Foster, P.; Adams, D.; Carroll, D.C.; Dromey, B.; Hawkes, S.; Kar, S.; Li, Y.T.; Markey, K.; McKenna, P.; et al. Spectral modification of laser-accelerated proton beams by self-generated magnetic fields. *New J. Phys.* **2009**, *11*, 083108. [CrossRef]
24. Nakatsutsumi, M.; Sentoku, Y.; Korzhimanov, A.; Chen, S.N.; Buffechoux, S.; Kon, A.; Atherton, B.; Audebert, P.; Geissel, M.; Hurd, L.; et al. Self-generated surface magnetic fields inhibit laser-driven sheath acceleration of high-energy protons. *Nat. Commun.* **2018**, *9*, 280. [CrossRef] [PubMed]
25. Huang, H.; Zhang, Z.M.; Zhang, B.; Hong, W.; He, S.K.; Meng, L.B.; Qi, W.; Cui, B.; Zhou, W.M. Investigation of magnetic inhibition effect on ion acceleration at high laser intensities. *Matter Radiat. Extrem.* **2021**, *6*, 044401. [CrossRef]
26. Surmin, I.A.; Bastrakov, S.I.; Efimenko, E.S.; Gonoskov, A.A.; Korzhimanov, A.V.; Meyerov, I.B. Particle-in-Cell laser-plasma simulation on Xeon Phi coprocessors. *Comput. Phys. Commun.* **2016**, *202*, 204–210. [CrossRef]
27. Gurevich, A.V.; Pariiskaya, L.V.; Pitaevskii, L.P. Self-similar motion of rarefied plasma. *Sov. Phys. JETP* **1966**, *22*, 449–454.
28. Mora, P.; Pellat, R. Self-similar expansion of a plasma into a vacuum. *Phys. Fluids* **1979**, *22*, 2300–2304. [CrossRef]

29. Hakobyan, H.; Philippov, A.; Spitkovsky, A. Effects of Synchrotron Cooling and Pair Production on Collisionless Relativistic Reconnection. *Astrophys. J.* **2019**, *877*, 53. [CrossRef]
30. Hakobyan, H.; Petropoulou, M.; Spitkovsky, A.; Sironi, L. Secondary Energization in Compressing Plasmoids during Magnetic Reconnection. *Astrophys. J.* **2021**, *912*, 48. [CrossRef]